Eur. Phys. J. B **38**, 437–444 (2004)
DOI: 10.1140/epjb/e2004-00137-6

THE EUROPEAN PHYSICAL JOURNAL B

Energetics of native point defects in cubic silicon carbide

F. Bernardini, A. Mattoni, and L. Colombo[a]

INFM and Department of Physics University of Cagliari, Cittadella Universitaria, 09124 Monserrato (CA), Italy

Received 9 January 2004
Published online 28 May 2004 – © EDP Sciences, Società Italiana di Fisica, Springer-Verlag 2004

Abstract. In this work we present a detailed investigation of native point defects energetics in cubic SiC, using state-of-the-art first principles computational method. We find that, the carbon vacancy is the dominant defect in p-type SiC, regardless the growth conditions. Silicon and carbon antisites are the most common defects in n-type material in Si-rich and C-rich conditions respectively. Interstitial defects and silicon vacancy are less favorite from the energetic point of view. The silicon vacancy tends to transform into a carbon vacancy-antisite complex and the carbon interstitial atom prefers to pair to a carbon antisite. The dumbbell structure is the lowest-energy configuration for the isolated carbon interstitial defect, and the tetrahedral interstitial silicon is a stable structure in p-type and intrinsic conditions, while in n-type material the dumbbell configuration is the stable one. Our results suggest that, in samples grown in Si-rich stoichiometric conditions, native defects are a source of n-doping and of compositional unbalance of nominally intrinsic SiC, in accord with experimental evidence.

PACS. 61.72.Ji Point defects (vacancies, interstitials, color centers, etc.) and defect clusters – 68.55.Ln Defects and impurities: doping, implantation, distribution, concentration, etc. – 74.62.Dh Effects of crystal defects, doping and substitution

1 Introduction

Silicon carbide is a group-IV compound material with a paramount importance for electronic, structural or nuclear applications. It exists in a variety of closed-packed arrangements or polytypes, the most common ones being the cubic (zincblende) 3C-SiC and the hexagonal 6H-SiC structure. Furthermore, the chemical similarity of Si and C atoms allows for the formation of non-stoichiometric disordered Si_xC_{1-x} solid solutions. Among those solid solutions ideal zincblende SiC represents a special and very stable structure. Experimental analysis of lattice constant and density indicates that 3C-SiC is indeed non-stoichiometric and Si-rich [1]. Moreover electrical measurements show that "as-grown" SiC is weakly n-type [2]. Those findings suggest that native lattice defects (like silicon antisites, carbon vacancies and silicon interstitials) play an important role in determining the actual composition and electronic properties of SiC.

Several authors investigated the electronic structure and thermodynamics of defects in SiC using ab initio or tight-binding semi-empirical techniques, focusing their attention on a subset of possible defects, mainly vacancies [3,4] and antisites [5], or limiting their investigation to neutral defects [6]. Other works have been addressed to selected electronic properties of these defects, as the hyperfine tensor [7]. Some investigations made use of drastic approximations on the computation of the electronic structure and therefore they cannot be considered any longer as accurate state-of-the-art calculations [8,9].

Noticeable exceptions are references [10–14], where an overall picture of the energetics of point defects in SiC is given. Unfortunately, in reference [10] very small supercells (32 atoms) have been used in the calculation, therefore the reliability of the results is somewhat questionable. In other works [11–14] a great deal of attention was devoted to those aspects of defect physics relevant for diffusing mechanism in SiC, nevertheless a comprehensive database of the formation energy for all of the defects considered is there missing.

In this work we provide a complete and consistent picture of defects in SiC. In particular we propose a methodological approach especially designed to study those defects with ionization levels in the upper part of the conduction band gap, whose investigation is somewhat problematic within the framework of the density functional theory (DFT).

2 Method

2.1 Supercell approach

The formation energies of point defects have been computed using the standard formalism by Zhang and Northrup [15]. We define the formation energy

[a] e-mail: luciano.colombo@dsf.unica.it

$\Delta H_{\rm form}(D^Q)$ for a defect D in the charge state Q as

$$\Delta H_{\rm form}(D^Q) = E_{\rm tot}(D^Q) - \sum_X n_X \mu_X + Q(\mu_e + E_{\rm v}) + M(Q), \quad (1)$$

where μ_e is the electron chemical potential (equaling the Fermi level E_F in our $T = 0$ K calculations), $E_{\rm tot}(D^Q)$ is the total energy of the defective supercell in charge state Q, $E_{\rm v}$ its top valence band energy, $M(Q)$ the defect-dependent multipole corrective term of reference [16], $n_{\rm X}$ and $\mu_{\rm X}$ the number of atoms of the species involved (X = C, Si) and their chemical potentials, respectively. The chemical potential of C and Si ($\mu_{\rm C}$ and $\mu_{\rm Si}$) are not independent variables, since both species are in equilibrium with SiC bulk compound. Therefore $\mu_{\rm C}$ and $\mu_{\rm Si}$ must satisfy the following condition:

$$\mu_{\rm SiC}^{\rm bulk} = \mu_{\rm C} + \mu_{\rm Si}. \quad (2)$$

Furthermore each chemical potential has to be lower than its bulk value in order to inhibit phase separation, namely

$$\mu_{\rm C,Si} < \mu_{\rm C,Si}^{\rm bulk} \quad (3)$$

so that we can express the formation energy of a defect as a function of one chemical potential only

$$\Delta H_{\rm form}(D^Q) = E_{\rm tot}(D^Q) - n_{\rm C}\mu_{\rm SiC}^{\rm bulk} - (n_{\rm Si} - n_{\rm C})\mu_{\rm Si} + Q\,(\mu_e + E_{\rm v}) + M(Q) \quad (4)$$

where

$$\mu_{\rm SiC}^{\rm bulk} - \mu_{\rm C}^{\rm bulk} \le \mu_{\rm Si} \le \mu_{\rm Si}^{\rm bulk}. \quad (5)$$

Total energies and bulk chemical potentials are computed within the local density functional theory following the parameterization of Perdew and Zunger [17] to the exchange-correlation functional, using ultra-soft pseudopotentials [18] and the plane-waves code provided in the VASP package [19]. As for the bulk chemical potential of Si and C we use their calculated value in the diamond structure at their theoretical equilibrium values.

We simulate an isolated defect within periodic boundary conditions via the repeated supercell approach. We use a very large $3\times3\times3$ supercell of cubic shape encompassing 216 atoms for all of the defects examined here. To manage those large supercells we used a very soft C pseudopotential available within VASP package. This pseudopotential gives a very good description of important bulk properties of SiC, like heat of formation that perfectly matches the experimental value of -0.66 eV/formula-unit [20] and lattice parameter (4.312 Å) in good agreement with the experimental value 4.360 Å [21]. A plane-wave cutoff of 211 eV is used throughout our calculations. As a further check we compared the formation energy for the fully relaxed vacancies and antisites here investigated using two different C atom pseudopotentials in a $2 \times 2 \times 2$ supercells. We estimated that the error induced by the use of a soft pseudopotential on the defects formation energies is at most 0.2 eV.

2.2 Reciprocal space sampling

Supercells size and BZ sampling are crucial aspects of accurate point defects calculations. Ideally a defect energy calculation within the periodic boundary conditions (PBC) would require a supercell large enough to insure that (i) the interaction among the periodic images of the defect is negligible, (ii) the total energy for the supercell is independent of the **k** point sampling used in the calculations. However, even for the largest supercells used in actual first-principles calculations, the interaction among defect images is not negligible and BZ sampling is not a matter of trivial choice. The crucial point is that within PBC, the interaction between periodic images causes a dispersion of the defect levels in the gap. Consequently, we have to deal with defects bands rather that with defects levels. Defects bands do not faithfully preserve the properties of their corresponding defects levels. Remarkably, defects bands do not have the same degeneracy of defects levels. The loss of degeneracy leads to an erroneous occupation of the defects states; indeed, according to the rules for level occupation in semiconducting materials, different occupations will be attributed to those state of the multiplets originated form the split of an otherwise degenerate defect level. Moreover the energy split among the multiplet states are added in the band structure term of the total energy. It is clear that as a consequence, erroneous charge distributions and total energies may be obtained with this procedure. A detour to avoid this unphysical effect is to restrict the BZ sampling to the Γ-point alone, where the degeneracy of defect levels is preserved. This choice has two drawbacks, namely even for large supercells (216 atoms) bulk-like properties are poorly converged for a Γ-point sampling calculation, and at the *supercell* Γ-point the conduction band energy is grossly underestimated because of the well-known DFT band gap problem. As a consequence those defects whose ionization levels are higher than the DFT band gap and lower than the actual material band gap, will appear above the conduction band minimum. This effect makes problematic the attribution of the correct occupation for the eigenstates, since it is not easy to disentangle the proper extrinsic level from the bulk band structure background. Customary the solution of the band gap problem is in the use of a set of special **k** points that avoids the BZ central region, typically a $2 \times 2 \times 2$ Monkhorst-Pack set. For this kind of sampling a satisfactory convergence of the bulk environment is achieved but the above mentioned problem of the defects levels degeneracy remains unsolved.

Summarizing a proper choice of the BZ sampling would require a set where at each k point: (i) the defects levels degeneracy is preserved, as at the Γ point, (ii) the conduction band energy is high enough that DFT band gap underestimation does not constitute a problem, (iii) the set provides a good convergence of the total energy with respect to the size of the supercell used.

In this work we use a procedure that circumvents both the degeneracy problem and the band gap DFT underestimation. Makov et al. [22] have shown that for the calculation of aperiodic systems (e.g. isolated defects), it exists

an optimal set of **k** points. In the specific case of cubic supercells, it consists of the high-symmetry Γ and R point. The use of this set allows the cancellation of those terms in the total energy arising from the interaction of adjacent periodic images, greatly improving the convergence of the formation energy with respect to the supercell size. In our specific case the use of this two-point set warrants that at the R point the actual degeneracy of the defect levels is preserved (as in the Γ point); furthermore, at the R point the conduction band is high enough, so that the DFT band gap underestimation does not represent a problem. Since we have to attribute to the eigenstates at Γ a proper occupation we device the following procedure. We start with a trial calculation of the supercell electronic structure with the **k** points set suggested in reference [22]. We inspect the eigenspectrum at R and identify the presence of defects levels in the band gap. We explore the band structure at Γ and identify the position of the same levels with respect to the bulk band structure. If the occupied levels lie below the conduction band minimum at Γ we choose the occupation at Γ to be the same as at the R point. If we find the level at Γ to be above the conduction band we set the occupation numbers so that the conduction band states at Γ are empty and the defect levels is properly occupied according to the total number of electrons. At first this procedure could look somewhat cumbersome, especially because of the need to set by hand the occupation numbers, instead to rely on Fermi-Dirac or Methfessel-Paxton [23] distribution functions. In reality for supercells as large as our (216 atoms) we found easy to identify the nature of the eigenstates at Γ from the knowledge of the band structure at the R point. This procedure offers moreover the additional advantage that occupation numbers of a given band do not vary across the BZ.

2.3 Charged cell corrections

Another important aspect of defect calculations, is the proper evaluation of the formation energy for charged defects. The long-range nature of the electrostatic interaction requires the supercell to be a neutral system, therefore a compensating *jellium* background is added to neutralize the defect charge. Such a procedure of "neutralization" is still tricky, since, the total energy of the supercell will contain a terms due to the *jellium*-defect interaction that is absent in the actual system. This term is a non negligible component even for very large supercells, therefore accurate calculation require that this source of error is properly handled. Historically two approaches have been used to correct the formation energy for the effect of the neutralization: the average potential correction and the so called Madelung correction.

Within the first method [25], the electron chemical potential μ_e is referred to a charge dependent valence band maximum E_v^Q defined as:

$$E_v^Q = E_v(\text{bulk}) + \left[V_{ave}^Q(\text{defect}) - V_{ave}(\text{bulk})\right] \quad (6)$$

where $V_{ave}(\text{defect})$ is the average potential far from the defect center in the supercell and $V_{ave}(\text{bulk})$ the corresponding value in the ideal bulk supercell. Accordingly in this approach the defect formation energy is written as:

$$\Delta H_{\text{form}}(D^Q) = E_{\text{tot}}(D^Q) - \sum_X n_X \mu_X + Q\left(\mu_e + E_v^Q\right). \quad (7)$$

In the second approach [16] an explicit correction for the formation energy $M(Q)$ is given. Its value in the case of a cubic supercell of side length L is:

$$M(Q) = \frac{Q^2\alpha}{2L} + \frac{2\pi Q q}{3L^3} \quad (8)$$

where α is the Madelung constant for the supercell lattice and q is the quadrupole moment of the defect charge. In literature both methods have been employed in the calculation of defects formation energies in SiC, in references [3–5] the average potential correction was used while in reference [26] the Madelung correction is used. We note that, in general, works dealing with wurtzite structure SiC employ the average potential correction since the implementation of the quadrupole moment corrective term of equation (8) is extremely cumbersome for hexagonal structure crystals. In this work we choose to employ the latter as a standard procedure and critically discuss the, somewhat sizable, differences in the results obtained with the former. We find that a proper correction of the periodic images interaction for charged defects is the most important aspect of a well-converged calculation.

2.4 Jahn-Teller effect

A last but not less important methodological aspect of our calculations is the proper choice of the occupation numbers for degenerate states. It is known that defects with partially filled degenerate states undergo to symmetry lowering distortions called Jahn-Teller (JT) effect. This effect splits a degenerate level into a multiplet with an upper empty (or nearly empty) and a lower filled (or partially filled) branch. Such kind of distortions are very difficult to reproduce by first-principles calculation because of the very low energy gain normally involved in the symmetry lowering distortion. We performed test calculations to understand if technical aspects of the present calculation can be responsible for the absence or the underestimation of existing JT effect. We found that the occupation of the defect level in its initial configuration plays an important role. As stated above we used for the BZ sampling two high-symmetry points where the actual degeneracy of the isolated defect is preserved. Therefore, in the high symmetry configuration an arbitrary choice of the occupation numbers for the defect level is possible. We can decide to distribute the occupation uniformly on the eigenstates contributing to the degenerate level according to finite temperature smearing distributions or to attribute to the lower eigenstate(s) full occupation and leaving the others empty. We find that the outcome of the calculation is very

different. Indeed, starting from a uniform occupation and a slightly distorted defect geometry we do not get any important symmetry lowering distortion, while for non-uniform occupations a sizeable distortion and a substantial gain of energy is obtained. These tests suggest that JT distortions can be properly computed only if a non-uniform occupation is attributed to degenerate (or nearly degenerate) levels.

3 Results

3.1 Overall picture

We investigated eight kinds of native defects, namely carbon vacancy (V_C), silicon vacancy (V_{Si}), silicon antisite (Si_C), carbon antisite (C_{Si}), interstitial silicon (Si_I), interstitial carbon (C_I), the complex formed by a carbon vacancy and a carbon antisite (V_C-C_{Si}), a carbon interstitial paired to a carbon antisite (C_I-C_{Si}). In the case of the vacancies and antisites the geometric structure of the defect is straightforward. As for interstitials, the identification of the minimum energy configuration is not as easy. Indeed the search for the stable structure for the interstitial atoms goes through the comparison of different candidate geometries. An exhaustive work would imply a search for several local minimum energy configurations (i.e. tetrahedral, hexagonal, bond-center, dumbbell). The ensemble of these configurations is very large; here we limited our investigation to tetrahedral and dumbbell configurations. We rule out the hexagonal interstitial because it is found to be an unstable configuration [12] and the bond-center because it is a geometry usual of small monovalent and divalent atoms (e.g. hydrogen and oxygen). A tetrahedral interstitial atom has two possible geometries, depending on the arrangement of the neighboring atoms: the TS configuration (where the interstitial atom is surrounded by four silicon atoms) and the TC configuration (where neighbors are carbon atoms). The dumbbell interstitial is a more complex structure where two atoms share the same lattice site: one is the atom that initially occupied that position and the other is the real interstitial species. Four kind of dumbbell interstitials are possible: two are C_I-Si and Si_I-Si pairs centered on Si sites; the other two ones are C_I-C and Si_I-C centered on C sites, where subscript I indicates the interstitial species. The inclusion in the present investigation of dumbbell interstitials is motivated by the results obtained in references [6,12], suggesting that interstitial atoms prefer dumbbell configurations.

We show our results in Table 1 and in the form of a diagram in Figures 1 and 2 for the Si-rich and C-rich conditions respectively. For the specific choices of the pseudopotentials used in this work the values of the chemical potentials for silicon (carbon) in Si-rich and C-rich stoichiometric conditions corresponds to −5.97 (−10.73) eV and −6.63 (−10.07) eV respectively. Besides the differences in the formation energies of the defects between Si-rich and C-rich conditions, we find common trends in the behavior of the defects we investigated.

Table 1. Charge states, range of stability, and formation energy (units of eV) for the defects studied. For each defect and charge state considered in this work we show the lower and upper bound for the electron chemical potential μ_e(min/max) and the corresponding formation energies $\Delta H_{\rm form}(D^Q)$ in Si-rich and C-rich stoichiometric conditions.

Defect	$\mu_e^{\rm min}$	$\mu_e^{\rm max}$	$\Delta H_{\rm form}(D^Q)$	
			Si-rich	C-rich
V_C^{2+}	0.00	1.32	1.20/3.84	1.86/4.50
V_C^{0}	1.32	2.40	3.84	4.50
V_{Si}^{1+}	0.00	0.41	8.37/8.78	7.71/8.12
V_{Si}^{0}	0.41	0.88	8.78	8.12
V_{Si}^{1-}	0.88	1.40	8.78/8.26	8.12/7.60
V_{Si}^{2-}	1.40	1.89	8.26/7.28	7.60/6.62
V_{Si}^{3-}	1.89	2.15	7.28/6.49	6.62/5.83
V_{Si}^{4-}	2.15	2.40	6.49/5.51	5.83/4.85
C_{Si}^{0}	0.00	2.40	4.15	2.83
V_C-C_{Si}^{2+}	0.00	1.23	4.26/6.71	3.60/6.05
V_C-C_{Si}^{1+}	1.23	1.76	6.71/7.24	6.05/6.58
V_C-C_{Si}^{0}	1.76	2.40	7.24	6.58
Si_C^{1+}	0.00	0.13	3.53/3.66	4.85/4.98
Si_C^{0}	0.13	2.40	3.66	4.98
C_I-C_{Si}^{2+}	0.00	0.81	6.02/7.64	4.02/5.64
C_I-C_{Si}^{0}	0.81	1.54	7.64	5.64
C_I-C_{Si}^{2-}	1.54	2.40	7.64/5.91	5.64/3.91
C-Si$\langle 100\rangle^{2+}$	0.00	0.81	5.71/7.31	5.05/6.65
C-Si$\langle 110\rangle^{0}$	0.81	1.81	7.31	6.65
C-Si$\langle 110\rangle^{1-}$	1.81	2.16	7.31/6.96	6.65/6.30
C-Si$\langle 110\rangle^{2-}$	2.16	2.40	6.96/6.48	6.30/5.82
Si-C$\langle 110\rangle^{4+}$	0.00	1.43	3.52/9.22	4.18/9.88
Si-C$\langle 110\rangle^{3+}$	1.43	1.71	9.22/10.06	9.88/10.72
Si-C$\langle 110\rangle^{2+}$	1.71	1.99	10.06/10.63	10.72/11.29
Si-C$\langle 110\rangle^{1+}$	1.99	2.22	10.63/10.86	11.29/11.52
Si-C$\langle 110\rangle^{0}$	2.22	2.40	10.86	11.52

First of all, the carbon vacancy together with the silicon and carbon antisites are the dominant defects in SiC. The silicon interstitial defect has an high formation energy and does not play an important role in SiC grown in equilibrium thermodynamic conditions. As for the V_C-C_{Si} and C_I-C_{Si} complexes, their concentrations are low, and their role as a donating defects is marginal. There is also a tendency of the defects to be electron donors. Those accepting electrons, (i.e. the silicon vacancy, the carbon interstitial and the carbon interstitial-antisite complex) have a formation energy higher than that of the donors for most of the allowed range of the electron chemical potential. As for antisites and vacancies, those ones associated with an excess of silicon are favored over their carbon rich counterpart. An exception is represented by the carbon antisite in C-rich conditions. Finally, we find that the tetrahedral interstitial is always energetically unfavored with respect to the formation of dumbbell configurations or interstitial-antisite complexes, the sole exception represented by the fourfold donor silicon interstitial defect.

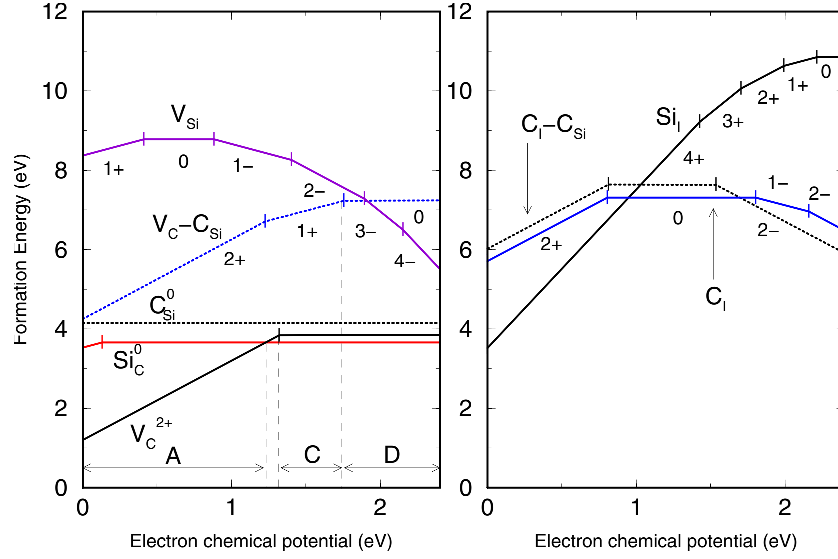

Fig. 1. Formation energy of native point defects in 3C-SiC (Si-rich conditions). The charge states for the defects are shown explicitly and the ionization levels are marked by a vertical bars. Left panel: Vacancies, antisites and V_C-C_{Si} complex. Right panel: Carbon, silicon interstitials and C_I-C_{Si} complex.

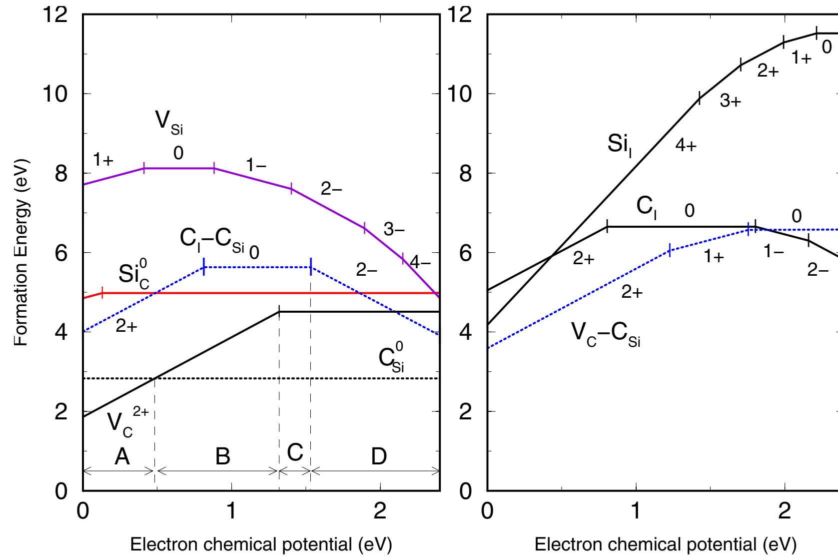

Fig. 2. Formation energy of native point defects in 3C-SiC (C-rich conditions). Same notation as in Figure 1 is used. Left panel: Vacancies, antisites and C_I-C_{Si} complex. Right panel: Carbon, silicon interstitials and V_C-C_{Si} complex.

We divided the diagrams in Figures 1 and 2 in four regions (labeled A,B,C and D respectively) with common features. Region A spans over an interval 1.23 (0.48) eV wide in Si-rich (C-rich) conditions. In this region V_C^{2+} is the dominant defect. Its formation energy varies from 1.20 (1.86) eV to 3.66 (2.83) in Si-rich (C-rich) growth conditions. These results indicate that especially in Si-rich growth conditions, p-type doping of SiC is compensated by the formation of double donor carbon vacancies. Region B refers to the conditions where the antisites are the lowest energy defects and V_C^{2+} is the next lower energy defect. This region is very wide in C-rich SiC (from 0.48 to 1.32 eV above E_v) because of the low formation energy for C_{Si}, and it is virtually absent in Si-rich SiC; intrinsic and lightly n-type material falls in this region. Region C spans over an interval where the lowest energy non neutral defect is the V_C-C_{Si} complex. The width of this region depends on the stoichiometry at growth. In C-rich SiC, the formation energy for C_I-C_{Si} is lower than that of V_C-C_{Si} and therefore region C extends up to the 0/2− ionization level of C_I-C_{Si}. In Si-rich SiC, the V_C-C_{Si} complex is lower in energy and region C extends up to the 1+/0 ionization level of V_C-C_{Si}. Finally, region D includes those part of the diagram where the dominant non neutral defects are acceptors. In this region n-type doping may be partially compensated by a light background of acceptors.

The identity of those defects depends on the material stoichiometry, in Si-rich conditions V_{Si} is the dominant defect while, in C-rich conditions the $\mathrm{C_I}$-$\mathrm{C_{Si}}$ is the most common acceptor. Since those defects have a high formation energies n-type doping of SiC is not affected by relevant self-compensation.

The results of our calculations suggests that intrinsic SiC is a lightly n-type material, with a Fermi level located just above the midgap, near the boundary between region B and C. Indeed, the existence of donating V_{C}^{2+} will push E_F above its midgap value near the 2+/0 ionization level. In region C the sole donors are the V_{C}-$\mathrm{C_{Si}}$ complex and the silicon interstial defect, whose concentration is too low to be effective as a source of free carriers. In the midgap region the formation energy of the carbon vacancy is ∼4 eV and its concentration is very low. On the base of pure equilibrium thermodynamics and of the values for the formation energy of our calculations we should conclude that native defects in SiC are responsible for a very low n-type doping whose concentration strongly depends on the material growth temperature. We point out that our calculations do not include the vibrational entropic term of the formation energy. We are not aware of any such calculation for the present material, we can only guess that the values of the entropy could be similar to those computed for the vacancy and interstitials in silicon [24], that is about 8 k_B in the case of the vacancy. Since SiC growth temperature can be as high as 2000 °C the effect of the entropic term would lower the formation energy of the vacancy by ∼2 eV. It is therefore hard to make a definitive assessment about the actual absolute concentration of free carriers in intrinsic SiC. Given the uncertainty on the concentration of these defects, we can say that our results are not in disagreement with the experimental evidence. The n-type character of nominally undoped SiC samples grown in Si-rich conditions [2] can be attributed (partially or totally) to the effect of the carbon vacancies. Moreover in intrinsic or n-type SiC samples ($E_F \geq 1.2$ eV) grown in Si-rich conditions, the dominant defects are V_{C} and $\mathrm{Si_C}$; both defects are responsible for the experimental evidence of silicon excess in most SiC samples [1]. We point out that our calculations predict that, in C-rich growth conditions, $\mathrm{C_{Si}}$ is the lowest energy defect for Fermi level above 0.48 eV. This finding implies that the experimental evidence of an excess of Si in as-grown material is not an unavoidable feature of SiC. On the contrary, it appears that the deviation from perfect stoichiometry in SiC is due to an unbalance between the chemical potential toward Si-rich conditions during the growth process.

3.2 Vacancies and antisites

The energetics of charged vacancies and antisites we present here is in general agreement with previous findings. Large supercells calculations for the vacancies were performed in references [3,4,12]. Our results for the carbon vacancy compares well with those of reference [3] both in the formation energy and in the ionization levels. In Figure 3 (left panel) we show that accounting for the JT distortion and the Madelung corrections (Eq. (1)), the carbon vacancy has a single ionization level 2+/0 at 1.32 eV. We notice that, according to the procedure of reference [25] (dashed line) the ionization level 2+/0, is located above the calculated conduction band at Γ (together with a second 0/2− ionization level), and its value is shifted down as a consequence of the Madelung correction. This finding shows that a correct choice for the occupation of the eigenstates is fundamental in this case. In reference [3] the problem was solved using a single $\mathbf{k}$ point sampling, which results from a $(2 \times 2 \times 2)$ Monkhorst-Pack mesh. The disadvantage of this choice is the loss of the actual defect level degeneracy, and the possible underestimation of the JT effect. Indeed in reference [3] the authors do not afford a direct calculation of the JT effect as a direct total energy difference calculations, but rely on an indirect estimation of the JT splitting, by means of an analytical nearest-neighbor vacancy tight-binding model. On the contrary here we perform a direct energy minimization, starting from a slightly distorted configuration and keeping the occupation constrained, as described in Section 3. The results of this procedure looks correct, in Figure 3, we show the results of the calculation for the tetrahedrally symmetric vacancy (dotted line). Our estimate for the JT energy gain for the neutral state is $\Delta E_{\mathrm{JT}} = 0.78$ eV favorably compares with the value of 1.13 eV reported in reference [3].

In Figure 3 (right panel) we show the formation energy for V_{Si} and V_{C}-$\mathrm{C_{Si}}$. The latter has been included in our calculation, since the results of reference [12] suggest that in p-type conditions V_{Si} is a metastable defect that converts into a V_{C}-$\mathrm{C_{Si}}$ complex. We find that our results for the silicon vacancy agree with those of reference [4] for the spin unpolarized system, while a sizable difference exists with reference [3]. As shown in Figure 3, the charge state of V_{Si} varies from 2+ to 4− as the electron chemical potential moves through the band gap. In reference [3] the lowest charge state is instead 2−. Therefore our results support the finding of reference [4] that a 4− charge state exists for the silicon vacancy. Furthermore, we agree with reference [26] that JT distortions are negligible in V_{Si}. Comparing the formation energy of V_{Si} and V_{C}-$\mathrm{C_{Si}}$ we confirm that V_{Si} is a metastable defect for charge states from 1+ to 2−. This has very important consequences for the properties of intrinsic SiC. In absence of this complex, V_{Si} would play the role of acceptor for E_F below 1.76 eV, instead, converting into V_{C}-$\mathrm{C_{Si}}$, the silicon vacancy becomes a donor, mimicking the role of the carbon vacancy. This insures that for electron chemical potentials below the 1+/0 ionization level of V_{C}-$\mathrm{C_{Si}}$, bulk SiC material is dominated by donor defects, i.e. intrinsic SiC has a residual n-type character.

Formation energies for the neutral antisites are in good agreement with the results of reference [5]. In these work a formation energy of 3.1 (4.3) eV is attributed to $\mathrm{C_{Si}^0}$ in C-rich (Si-rich) conditions that compares nicely with our estimated formation energy 2.83 (4.15) eV. A similar

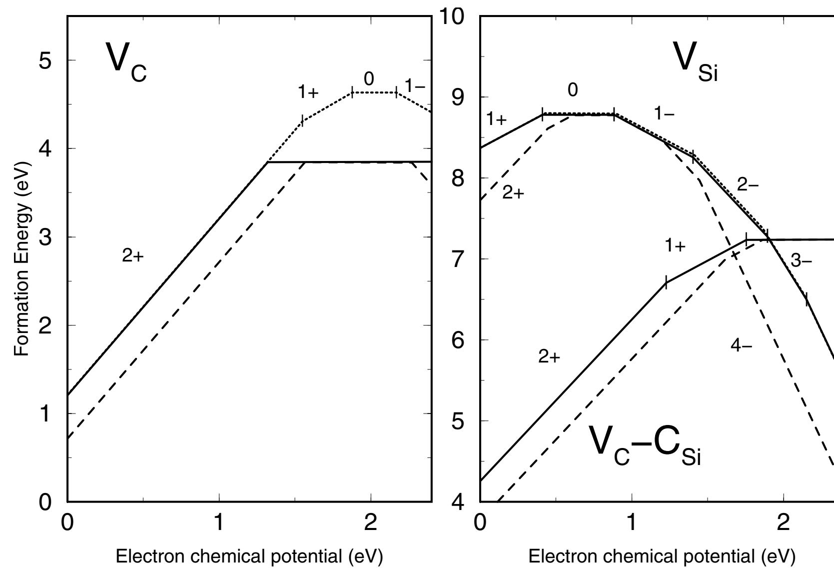

Fig. 3. Defects formation energies in the high symmetry tetrahedral geometry (dotted line) and after the Jahn-Teller distortion (solid line), computed using the Madelung correction of reference [16]. Same notation as in Figure 1 is used. The dashed line shows the formation energy for the Jahn-Teller low symmetry geometry computed using the average cell potential correction of reference [25]. Left panel: Carbon vacancy. Right panel: Silicon vacancy and V_C-C_{Si} complex.

satisfactory agreement is found for Si_C^0, their estimate of 4.0 (5.2) eV for the formation energy of Si_C^0 in Si-rich (C-rich) against our of 3.66 (4.98) eV. We find that in references [6,10] the formation energy of C_{Si} is underestimated while that of Si_C is overestimated. Indeed it would appear that the carbon antisite is the dominant defect in SiC, i.e. the material should have an intrinsic tendency to be rich in carbon. Conversely, our results show that stoichiometric conditions at the growth determine the relative balance between silicon and carbon antisites. In *p*-type conditions Si_C becomes a donor: we find that the charge state for Si_C varies from 1+ to 0, if Madelung correction are accounted for. This is at variance with the results of reference [5]. In that work the authors find that Si_C can donate up to four electrons. This difference is not surprising since ionization levels for Si_C are just above the valence band edge and slightly different technicalities of the calculation can account for it. Indeed in Figure 4 we show that computing the ionization levels by the average potential correction (Ref. [25]) we get results similar to those of reference [5], while using the Madelung corrections the ionization levels are shifted down and only the 1+/0 level survives. These findings put out that for defects with high charge state even calculation done for largest supercells used in this work are not yet totally at convergence.

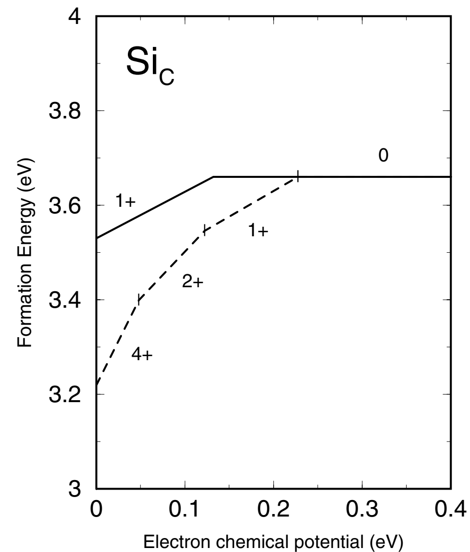

Fig. 4. Formation energy of a silicon antisite. Same notation as in Figure 1 is used. The data sets shown are computed using the Madelung correction of reference [16] (solid line) and the average cell potential correction of reference [25] (dashed line).

3.3 Interstitials

As for self-interstitial defects we investigated Si and C interstitials both in the tetrahedral sites (TS and TC) and dumbbell configuration. Furthermore, we investigated the stability and the charge states for the C_I-C_{Si} complex. The results of the calculations for the different configurations of a carbon interstitial defect are shown in Figure 5. We find that the carbon interstitial atom lowest energy structure is always a dumbbell configuration, while the tetrahedral configuration is energetically strongly unfavorable. In the 2+ charge state the dumbbell is a $\langle 100\rangle$-oriented carbon atom pair substituting at a carbon site (C_I-$C\langle 100\rangle^{2+}$). For the other charge states the preferred configuration is a strongly asymmetric C_I-Si dumbbell. The latter is a low symmetry structure, with the silicon-carbon pair lying in the $[1\bar{1}0]$ plane, where the silicon atom is very near to the ideal lattice site and the dimer axis direction is intermediate between the $\langle 111\rangle$ and the $\langle 110\rangle$. In Figure 5

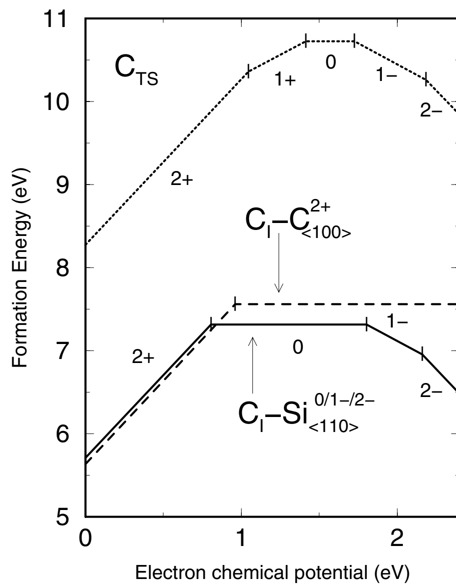

Fig. 5. Formation energy of a carbon interstitial atom in SiC (Si-rich conditions). Same notation as in Figure 1 is used. Tetrahedral geometry (dotted line), ⟨100⟩-oriented dumbbell (solid line) and ⟨110⟩-oriented dumbbell (dashed line).

for brevity we refer to this configuration as a C_I-Si⟨110⟩ interstitial.

For the silicon interstitial atom too the actual configuration depends on charge state. In this case we find that the competing configurations are the tetrahedral interstitial and the low symmetry Si_I-C⟨110⟩ dumbbell. For E_F below 1.42 eV, the silicon atom sits at the TC interstitial site and it behaves as a donor, releasing four electrons. For higher Fermi levels the tetrahedral site is no more a stable configuration and spontaneously converts into the low symmetry Si_I-C⟨110⟩ dumbbell interstitial, whose geometry has been already described for the carbon interstitial. We point out that in the case of the silicon interstitial tetrahedral and dumbbell configurations are very similar in energy, within an interval of 0.15 eV, possibly beyond the accuracy of the present calculations.

4 Conclusions and acknowledgments

In conclusion, in this work we have investigated the most relevant native point defects in 3C-SiC. We conclude that V_C, Si_C and C_{Si} are the dominant defects in SiC. V_C is always the lowest energy defect in p-type SiC regardless the value of the μ_{Si} and μ_C. In p-type and semi-insulating SiC, V_{Si} is a metastable defects that converts exotermically into a V_C-C_{Si} complex. V_C and V_C-C_{Si} are the possible source of the experimental detected n-type character of intrinsic SiC. Our results show that the excess of silicon typical of SiC samples is a consequence of Si-rich stoichiometric conditions at growth. We confirm that carbon interstitial atoms minimum energy configuration is a dumbbell structure, while for the silicon interstitial dumbbell and tetrahedral interstitial configurations are very similar in energy.

This work has been funded by MIUR PRIN-2002 project "Fracture mechanics in complex covalently-bonded materials". We acknowledge computational support by INFM under "Parallel Computing" Initiative.

References

1. K.L. More, J. Ryu, C.H. Carter, J. Bentley, R.F. Davis, Cryst. Lattice Defects Amorphous Mater. **12**, 243 (1985)
2. H.J. Kim, R.F. Davis, J. Electrochem. Soc. **133**, 2350 (1986)
3. A. Zywietz, J. Furthmüller, F. Bechstedt, Phys. Rev. B **59**, 15166 (1999)
4. L. Torpo, R.M. Nieminen, K.E. Laasonen, S. Pöykkö, Appl. Phys. Lett. **74**, 221 (1999)
5. L. Torpo, S. Pöykkö, R.M. Nieminen, Phys. Rev. B **57**, 6243 (1998)
6. F. Gao, E.J. Bylaska, W.J. Weber, R. Corrales, Phys. Rev. B **64**, 245208 (2001)
7. M. Bockstedte, M. Heid, O. Pankratov, Phys. Rev. B **67** 193102 (2003)
8. Y. Li, P.J. Lin-Chung, Phys. Rev. B **36**, 1130 (1987)
9. D.N. Talwar, Z.C. Feng, Phys. Rev. B **44**, 3191 (1991)
10. C. Wang, J. Bernholc, R.F. Davis, Phys. Rev. B **38**, 12752 (1988)
11. A. Mattauch, M. Bockstedte, O. Pankratov, Mater. Sci. Forum. **353-356**, 353 (2001)
12. M. Bockstedte, M. Heid, A. Mattausch, O. Pankratov, Mater. Sci. Forum. **389-393**, 471 (2002)
13. A. Mattausch, M. Bockstedte, O. Pankratov, Mater. Sci. Forum. **389-393**, 481 (2002)
14. M. Bockstedte, A. Mattausch, O. Pankratov, Phys. Rev. B **68**, 205201 (2003)
15. S.B. Zhang, J.E. Northrup, Phys. Rev. Lett. **67**, 2339 (1991)
16. G. Makov, M.C. Payne, Phys. Rev. B **51**, 4014 (1995)
17. J.P. Perdew, A. Zunger, Phys. Rev. B **23**, 5048 (1981)
18. D. Vanderbilt, Phys. Rev. B **41**, 7892 (1990)
19. G. Kresse, J. Hafner, Phys. Rev. B **47**, R558 (1993); G. Kresse, Thesis, Technische Universität Wien 1993; G. Kresse, J. Furthmüller, Comput. Mat. Sci. **6**, 15 (1996); G. Kresse, J. Furthmüller, Phys. Rev. B **54**, 11169 (1996)
20. D.D. Wangman, W.H. Evans, V.B. Parker, I. Halow, S.M. Baily, R.H. Schumm, *Selected Values of Chemical Thermodynamics Properties, Tables for the First Thirty-Four Elements in the Standard Order of Arrangements*, Natl. Bur. of Stand. Tech. Note No. 270-3 (U.S. GPO, Washington, D.C., 1968)
21. *Landolt-Börnstein: Numerical Data and Functional Relationships in Science and Technology,* edited by O. Madelung, New Series, Group III, Vol. 17a (Springer, Berlin, 1982), p. 49
22. G. Makov, R. Shah, M.C. Payne, Phys. Rev. B **53**, 15513 (1996)
23. M. Methfessel, A.T. Paxton, Phys. Rev. B **40**, 3616 (1989)
24. A. Jääskeläinen, L. Colombo, R. Nieminen, Phys. Rev. B **64**, 233203 (2001)
25. A. Garcia, J.E. Northrup, Phys. Rev. Lett. **74**, 1131 (1995)
26. L. Torpo, T.E.M. Staab, R.M. Nieminen, Phys. Rev. B **65**, 085202 (2002)
27. M. Yamanaka, H. Daimon, E. Sakuma, S. Misawa, S. Yoshida, J. Appl. Phys. **61**, 599 (1986)